CRYSTAL GROWTH & DESIGN

ARTICLE

pubs.acs.org/crystal

Interactions of Antithyroid Drugs and Their Analogues with Halogens and their Biological Implications

Published as part of a virtual special issue on Structural Chemistry in India: Emerging Themes

Gouriprasanna Roy, Krishna P. Bhabak, and Govindasamy Mugesh*

Department of Inorganic and Physical Chemistry, Indian Institute of Science, Bangalore 560012, India

Supporting Information

ABSTRACT: The selenium analogue of antithyroid drug methimazole (MSeI) reacts with molecular bromine to produce two different types of novel complexes depending upon the molar ratio of MSeI to Br_2 in the reaction medium. Dicationic diselenide complex with two Br^- ions as counterions is produced in the reaction of MSeI with 0.5 equiv of Br_2 (MSeI/Br_2, 1.0:0.5), whereas a stable 10-Se-3 hypervalent "T-shaped" complex featuring a linear Br−Se−Br moiety was produced when MSeI was treated with Br_2 in an equimolar ratio (MSeI/Br_2, 1.0:1.0). A substitution at the free N−H group in MSeI alters its reactivity toward iodine/bromine. For example, the *N*,*N*-disubstituted selones exclusively produce the corresponding 10-Se-3 hypervalent "T-shaped" complexes in the reaction with I_2. In the presence of the lectoperoxidase/H_2O_2/I^- system, *N*,*N*-dimethylimidazole-2-selone produces the corresponding dicationic diselenide with two I^- counterions as the final metabolite. The formation of ionic species in these reactions is confirmed by single crystal X-ray diffraction studies and in some cases by Fourier transform-Raman spectroscopic investigations.

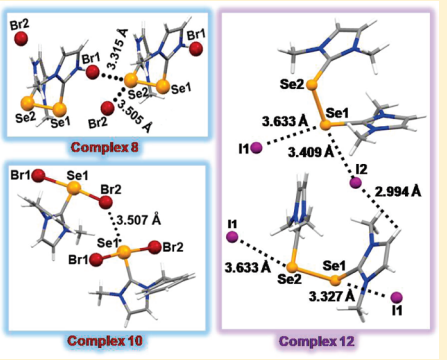

INTRODUCTION

The mechanism by which thiourea-based antithyroid drugs inhibit thyroid hormone biosynthesis has attracted considerable research interest for several years.[1−4] The initial studies have been focused on the inhibitory action of these compounds on the enzyme thyroid peroxidase (TPO), which is involved in the biosynthesis of thyroid hormones. Further insights into the thyroid system have also been provided by similar investigations on the effect of these compounds on other peroxidase enzymes such as lactoperoxidase (LPO), myeloperoxidase (MPO), and chloroperoxidase.[5−9] Although the inhibition of TPO and LPO by antithyroid agents has been extensively studied in recent years, the mechanism of inhibition of peroxidase-catalyzed oxidation and iodination reactions by these agents is still not clear. Several other mechanisms have been proposed for the inhibition of the biosynthesis of thyroid hormones.[1,3,10−13] For example, it has been proposed that TPO first undergoes an oxidation by H_2O_2 to the corresponding oxidized enzyme (TPO_{ox}), which interacts with the antithyroid agents. The resulting oxidized drugs may bind to the heme group of the enzyme, leading to an irreversible inactivation of the enzyme.[14−17] Biochemical studies also suggest that some of the thioureylene antithyroid drugs block the iodination in vivo by reducing the oxidized iodide generated by the TPO/H_2O_2/I^- system, which divert the iodide from the natural tyrosyl acceptor substrates.[18] Therefore, the molecular interactions of antithyroid drugs with iodine have been subjected to many investigations as these drugs may inhibit the thyroid hormone synthesis by forming donor−acceptor (D−A) complexes with iodine or interacting with an active iodine species of TPO. Furthermore, a number of in vitro experiments suggest that antithyroid drugs can form stable D−A complexes with diiodine (I_2) or oxidized iodine species (Figure 1) and thus divert oxidized iodides away from thyroglobulin (Tg).[19−21]

Recent studies on the reactions of selones (D) with dihalogen (X_2, A) suggest the possibility of the formation of different products:[22−28] (i) formation of neutral D−A charge-transfer (CT) complexes, in which donor atoms bind linearly with the X_2;[22] (ii) reaction of donor molecule with *n* number of acceptor molecules to form D−*n*A type CT complexes; (iii) formation of an X−D−X group by the homolytic cleavage of X−X bond (e.g., the hypervalent compounds of sulfur and selenium); (iv) formation of halonium salts, in which X^+ binds to two donor molecules in a linear fashion by heterolytic cleavage of the coordinated X−X molecule. As most of the heterocyclic thiones and selones exist as zwitterions, the CT complexes are formed by transfer of charge from a donor molecule (selone) to an acceptor molecule (X_2). This can be explained by a simplified molecular orbital (MO) theory description. Donation of a lone pair of electrons from the bonding orbital (HOMO) of donor to the σ^* antibonding LUMO orbital of X_2 accumulates a fractional negative charge on the σ^* orbital of the acceptor molecule.[29] This transfer of electron leads to an elongation of the X−X bond length in the X_2 molecule. The extent of charge transfer is generally measured either by monitoring the changes in ^{13}C NMR chemical shifts of the donor molecule or from the lowering of the ν(X−X) stretching vibration of X_2 by Fourier

Received: December 20, 2010
Revised: April 14, 2011
Published: April 19, 2011

transform (FT)-Raman spectroscopic analysis. A higher polarizability of selenium[30] as compared to sulfur leads to a better overlap of energies of the HOMO of selenium and the σ^* orbital of I_2. Therefore, selones generally provide relatively more stable D−A adducts with I_2 than the corresponding thiones. In this regard, the reactivity of thiourea-based antithyroid drugs and their selenium analogues toward I_2/Br_2 may significantly contribute to their antithyroid activities.

Recently, we have reported that the selenium analogue of antithyroid drug MMI (**2**, **MSeI**) reacts with molecular iodine to produce two different types of complexes (**6** and **7**) under different experimental conditions.[31] However, the effect of other halogens on the reactivity of these selenium analogues of antithyroid drugs has not been studied. Herein, we report some structural features of complexes obtained from the reaction of compound **2** with Br_2 instead of I_2 to understand the mode of reactivity of MSeI toward other halogens. In addition, the effect of free N−H group in the imidazole ring of MSeI on the reactivity toward halogen is described. As the antithyroid drugs have been shown to be oxidized by the TPO/H_2O_2 system, it is important to identify the metabolites obtained by reaction of antithyroid drugs with the TPO/H_2O_2/I^- system (model system) at physiologically relevant conditions for a better understanding of the mechanism of action in vivo.

RESULTS AND DISCUSSION

The reaction of **MSeI** (**2**) with bromine solution in dichloromethane afforded two different types of complexes (**8** and **9**) depending upon the molar ratio of **MSeI** to bromine. The reaction of **2** with 25 mol % of bromine in CH_2Cl_2 at 0 °C produced the corresponding dicationic diselenide with two Br^- as counterions (**8**) as orange crystals (Figures 1 and 2). It should be noted that complex **8** can also be synthesized by treating the diselenide **5** with a CH_2Cl_2 solution of bromine in a 1:1 molar ratio. Interestingly, addition of more than 25 mol % of bromine to **2** produced a different product. For example, addition of 50 mol % of bromine to compound **2** in CH_2Cl_2 at 0 °C produced a stable 10-Se-3 hypervalent "T-shaped" compound (**9**) featuring a linear Br−Se−Br moiety (Figure 1).[33]

As shown in Figure 2, complex **8** consists of a diselenide dication in which the two MSeI units are connected via a Se−Se bond. In the structure, the dication is stabilized by two Br^- counterions. As it can be seen from the X-ray crystal structure, one selenium atom (Se2) from each of the diselenide dications is involved in intermolecular interactions with two bromide ions (Br1 and Br2) of two adjacent molecular units [Se2···Br1 {−1 + x, y, z}: 3.315 Å and Se2···Br2 {1.5 − x, 1/2 + y, z}: 3.505 Å]. These intermolecular interactions assist the Se2 center of each diselenide unit to adopt distorted square planar coordination geometry (Figure 2B). Interestingly, the Se−Se bond length in complex **8** (2.3609(15) Å) is found to be almost similar to the Se−Se bond length observed in diselenide **5** (2.3569(14) Å), indicating a very weak intermolecular Se···Br interaction.[31,33] The C−Se bond lengths in complex **8** (1.890(9) and 1.898(9) Å) are also comparable to the corresponding C−Se bond length in compound **5** (1.882(3) Å). These observations suggest that the weaker Se···Br interactions and also the protonation of the nitrogen atoms in the imidazole ring of the diselenide do not affect the Se−Se bond length significantly. Complexes **8** and **9**

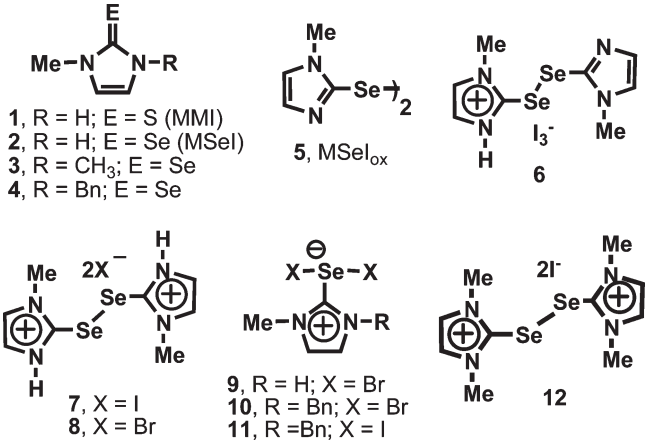

Figure 1. Chemical structures of antithyroid drug MMI, its selenium analogues, and their charge-transfer complexes.

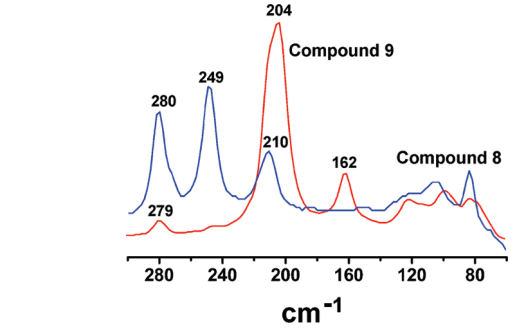

Figure 3. FT-Raman spectra of complexes **8** and **9**. Complex **8** shows Se−Se stretching vibrations at 280, 249, and 210 cm^{-1}. Complex **9** shows two strong peaks at 204 and 162 cm^{-1} for the Br−Se−Br three body system.

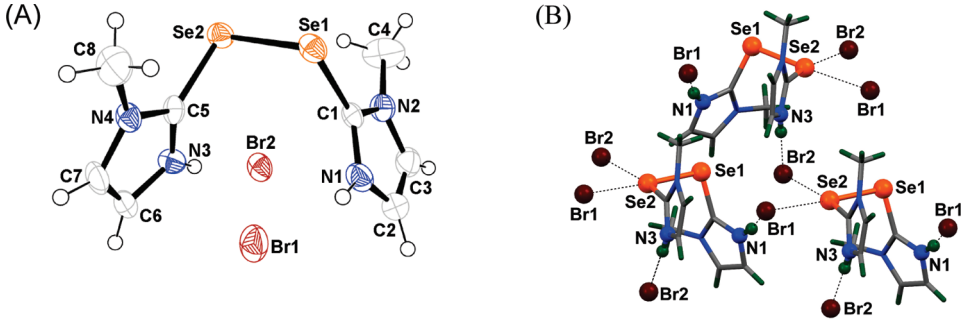

Figure 2. (A) ORTEP diagram of complex **8**, showing a diselenide dication stabilized by two Br^- ions. The thermal displacement ellipsoids are shown at the 50% probability level. (B) Molecular structure of complex **8** showing Se···Br contacts between the selenium atoms of dication with Br^- ions.

obtained from the reactions of **2** with Br_2 were further characterized by FT-Raman spectroscopy. Compound **8** exhibits three strong peaks at 280, 249, and 210 cm^{-1} in the FT-Raman spectrum, which can be ascribed to the ν(Se−Se) stretching vibrations. On the other hand, complex **9**, which does not contain any Se−Se bond, exhibited two strong bands at 204 and 162 cm^{-1}, which can be assigned to ν_{as} and ν_s of the Br−Se−Br three body system, respectively (Figure 3).

In addition to the intermolecular Se···Br interactions, Br^- ions in complex **8** are also involved in hydrogen bonding with the free N−H group of the adjacent imidazole unit as shown in Figure 2B. Both the Br^- ions are involved in the hydrogen bonding with the neighboring N−H groups, although the strength of two hydrogen bonds is slightly different (N1H···Br1: 2.420 Å; N3H···Br2: 2.374 Å). Notably, the Br^- ions form a bridge (NH···Br···Se) between two diselenide molecules by forming hydrogen bonding with one of the diselenide molecules and Se···Br noncovalent interaction with another molecule as illustrated in Figure 4. These noncovalent interactions facilitate the formation of a network structure (Figure 5).

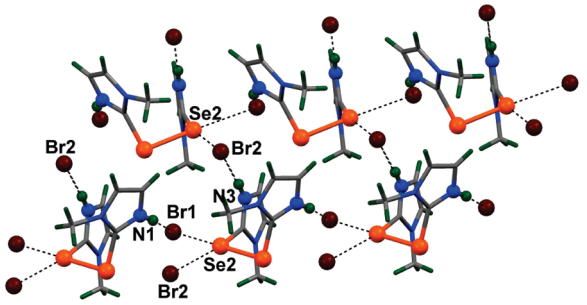

Figure 4. Chain-like structure of complex **8**. The Br^- ions form a bridge between two diselenide molecules by forming hydrogen bonding with free N−H group of one molecule and interaction with the Se atom of another molecule.

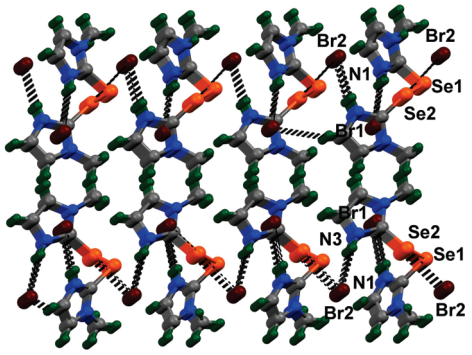

Figure 5. Packing diagram of complex **8** showing Se···Br and N−H···Br interactions.

We have shown previously that the reaction of **2** with I_2 in CH_2Cl_2 exclusively produces the corresponding monocationic diselenide **6** with I_3^- as counterion (Figure 1).[31] In contrast, the reactions of *N,N*-disubstituted selones **3** and **4** with I_2 afforded the corresponding T-shaped CT complexes as shown in Figure 1. Unlike compound **2**, the reaction of *N,N*-disubstituted selone **4** with Br_2 produced only the T-shaped adduct **10** (Figure 6). Dark red crystals of compound **10** were obtained from the reaction of selone **4** in CH_2Cl_2 solution of Br_2 (**4**:Br_2: 1:1). X-ray crystal structural analysis of the crystals confirmed the formation of "T-shaped" hypervalent selenium adduct **10** featuring an almost linear Br−Se−Br group [175.37(4)°], which is approximately perpendicular to the imidazole ring plane with a torsion angle of 71.90° (Br1−Se−C1−N2) (Figure 6).

Interestingly, the X-ray structure of compound **10** reveals that the two Se−Br bond lengths in the Br−Se−Br moiety are significantly different from each other [Se−Br1: 2.4940(12) Å and Se−Br2: 2.6976(12) Å]. The two C1−Se−Br bond angles are also found to be different from each other [C1−Se−Br1: 89.4(2)°; C1−Se−Br2: 86.0(2)°]. As expected, the longer Se−Br bond length [Se−Br2: 2.6976(12) Å] is associated with a smaller Se−Br bond angle [C1−Se−Br2: 86.0(2)°] as shown in Table 1. Similar to the selenium centers in complex **8**, the Se atom in complex **10** forms an approximately square planar geometry through a short interaction of the Se atom with the Br1 atom of an adjacent unit [Se···Br1 ($-x+1/2+1, +y-1/2, +z$) = 3.507 Å]. An expansion of the molecular units by considering the Se···Br1 interactions shows that complex **10** forms a zigzag shaped chain-like structure in which one molecule is attached to another molecule via Se···Br intermolecular interactions (Figure 7). It should be noted that complex **10** does not possess any intermolecular H-bonding interactions (Figure 7) due to the absence of a free N−H group in the imidazole ring. Therefore, the molecular network of **10** is formed mainly via Se···Br intermolecular interactions as shown in Figures 7 and 8.

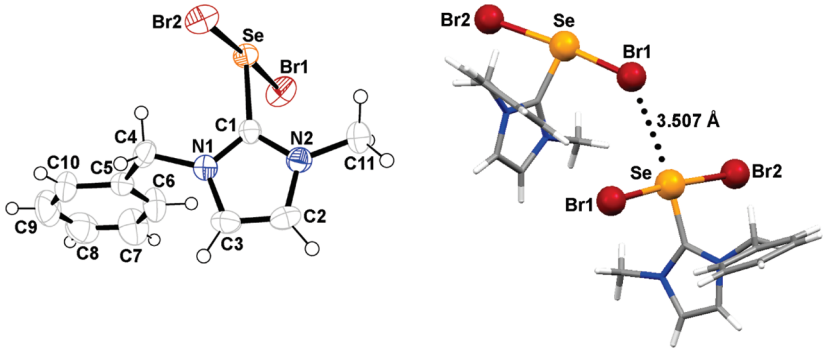

Figure 6. (Left) ORTEP diagram of the T-shaped adduct **10**. The thermal displacement ellipsoids are shown at the 50% probability level. (Right) Molecular structure of complex **10** showing Se···Br(1) contacts between the Se atom with Br atom of adjacent molecule [Se···Br1 ($-x+1/2+1, +y-1/2, +z$): 3.507 Å].

dx.doi.org/10.1021/cg101688v |*Cryst. Growth Des.* 2011, 11, 2279–2286

To understand the reactivity of selone **4** toward other halogens, this compound was treated with I_2 in a 1:1 molar ratio in CH_2Cl_2. A slow evaporation of the solvent afforded red color crystals of complex **11** as confirmed by single crystal X-ray diffraction studies. The structure of complex **11** revealed the formation of 10-Se-3 "T-shaped" hypervalent selenium adduct, which is similar to that of complex **10**.[35−38] These observations suggest that the reactivity of compound **4** toward I_2 is similar to that observed for Br_2. It should be mentioned that the reaction of **2** with I_2 in H_2O or in CH_2Cl_2 produced only the CT or ionic complexes **6** and **7**, whereas the reaction of **4** with I_2 generates only the "T-shaped" hypervalent selenium adduct. This clearly suggests that the substitution at the N−H group of the imidazole ring with benzyl group alters the reactivity of selones toward I_2. However, unlike complex **10**, the asymmetric unit of complex **11** contains two molecular units (Figure 9). The crystallographic parameters are shown in Tables 3 and 4. A detailed structural analysis reveals that both the molecular units in **11** possess linear I−Se−I moieties, which are almost perpendicular to the average molecular plane (imidazole ring). However, slight differences in the I−Se−I bond angles [I1−Se1−I2: 175.64(6)° and I1′−Se1′−I2′: 178.09(7)°] and I1−Se1−C1-N1 torsion angle [I1−Se1−C1−N1: 96.29°; I1′−Se1′−C1′−N1′: −100.95°] are observed between two molecular units in the asymmetric unit. Similar to compound **10**, it is observed that the two Se−I bond lengths in the I−Se−I moiety of compound **11** are significantly different from each other [Se1−I1: 2.8461(19) Å, Se1−I2: 2.7506(19) Å; Se1′−I1′: 2.7609(19) Å, Se1′−I2′: 2.8366(19) Å]. The Se1−I1 (2.8461(19) Å) and Se1′−I2′ (2.8366(19) Å) bond lengths are significantly longer than Se1−I2 (2.7506(19) Å) and Se1′−I1′ (2.7609(19) Å) bonds. The bond angles between C1−Se1−I1 (86.6(4)°) and C1−Se1−I2 (89.2(4)°) are close to 90° indicating that the I−Se−I moiety is oriented almost perpendicular to the imidazole ring plane. Interestingly, there is a good correlation between the C1−Se1−I bond angles and Se−I bond lengths; wider bond angles of C1−Se1−I are associated with shorter Se−I bond lengths (Table 2). Another interesting feature of compound **11** is that the Se center of one molecular unit forms a square planar geometry through noncovalent Se···I interactions with I atom of an adjacent molecule [Se1···I2′ ($x, -y + 1/2 + 1, +z + 1/2$) = 3.678 Å and Se1′···I1 ($x, -y + 1/2, +z - 1/2$) = 3.585 Å]. These Se···I interactions generate a zigzag shaped chain-like structure as shown in Figure 10. The C−Se bond lengths observed for C1−Se1 (1.887(12) Å) and C1′−Se1′ (1.897(13) Å) bonds are comparable to the C−Se single bond length, indicating the presence of a zwitterionic structure.

Table 1. Se−Br Bond Lengths (Å) and Bond Angles (°) of C(1)−Se−Br Unit in Complex 10

Se−Br1	2.4940(12)	N2−C2	1.387(10)
Se−Br2	2.6976(12)	N1−C3	1.374(10)
Se−C1	1.897(7)	C2−C3	1.344(12)
C1−N1	1.338(9)	C1−Se−Br1	89.4(2)°
C1−N2	1.334(9)	C1−Se−Br2	86.0(2)°

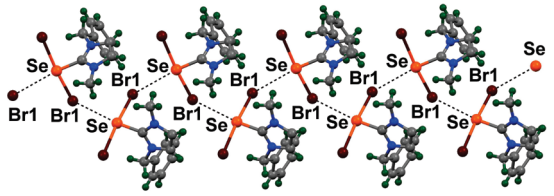

Figure 7. Chain-like structure of complex **10** showing Se···Br1 nonbonding interactions. The distance between Se and Br1 atoms is 3.507 Å [Se···Br1 ($-x + 1/2 + 1, +y - 1/2, +z$)].

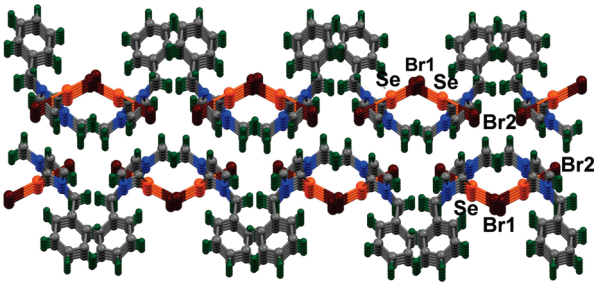

Figure 8. Packing diagram of complex **10** showing extensive Se···Br interactions.

Table 2. Se−I Bond Lengths (Å) and Bond Angles (°) between C(1)−Se−I of Complex 11

Se1−I1	2.8461(19) Å	C1−Se1−I1	86.6(4)°
Se1−I2	2.7506(19) Å	C1−Se1−I2	89.2(4)°
Se1′−I1′	2.7609(19) Å	C1′−Se1′−I1′	90.8(4)°
Se1′−I2′	2.8366(19) Å	C1′−Se1′−I2′	88.9(4)°

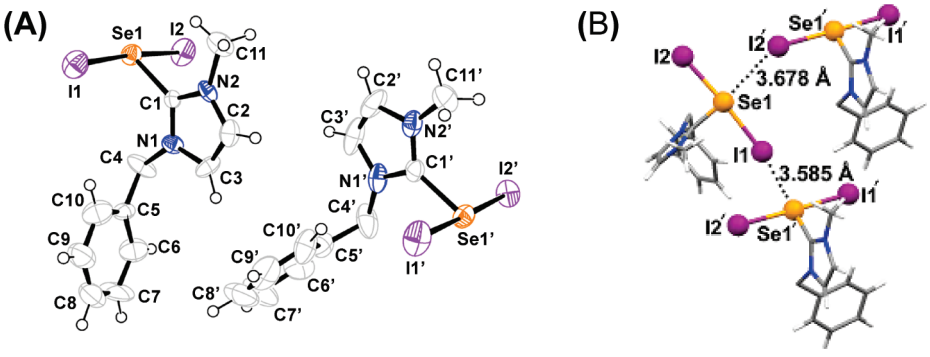

Figure 9. (A) ORTEP diagram of the T-shaped adduct **11**. The thermal displacement ellipsoids are shown at the 50% probability level. (B) Molecular structure of **11** showing Se···I contacts between the selenium atom of one molecule with iodine atom of the adjacent molecule [Se1···I2′ ($x, -y + 1/2 + 1, +z + 1/2$) = 3.678 Å and Se1′···I1 ($x, -y + 1/2, +z - 1/2$) = 3.585 Å].

dx.doi.org/10.1021/cg101688v |*Cryst. Growth Des.* 2011, 11, 2279–2286

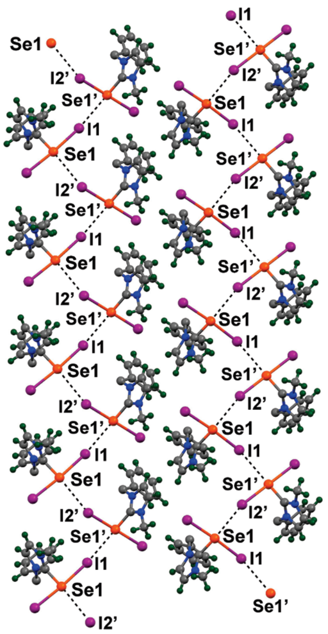

Figure 10. Chain-like structure of **11** showing Se···I intermolecular interactions. Contact distances between the selenium atom of one molecule with iodine atom of the adjacent molecule are Se1···I2′ $(x, -y + 1/2 + 1, +z + 1/2)$ = 3.678 Å and Se1′···I1 $(x, -y + 1/2, +z - 1/2)$ = 3.585 Å, respectively.

Table 3. Crystallographic Data for Compounds 8 and 10

	compound **8**	compound **10**
formula	$C_8H_{12}N_4Se_2Br_2$	$C_{11}H_{12}Br_2N_2Se$
F_w	481.96	411.01
crystal system	orthorhombic	orthorhombic
space group	*Pbca*	*Pbca*
a (Å)	7.0137(18)	11.207(2)
b (Å)	11.257(3)	8.1064(16)
c (Å)	35.392(9)	30.386(6)
α (°)	0.00	90.00
β (°)	90.00	90.00
γ (°)	90.00	90.00
V ($Å^3$)	2794.3(13)	2760.5(9)
D_{calc} (Mg m^{-3})	2.291	1.978
Z	8	8
μ (mm^{-1})	10.993	8.486
refl collected/unique	15802/3332	22207/3301
parameters	147	146
R_{int}	0.068	0.064
R (observed data)[a]	R_1 = 0.053; wR_2 = 0.154	R_1 = 0.042; wR_2 = 0.125
R (all data)[b]	R_1 = 0.094; wR_2 = 0.198	R_1 = 0.084; wR_2 = 0.185
goodness-of-fit on F^2	0.688	0.558
$\Delta\rho_{min}$ and $\Delta\rho_{max}$ (e $Å^{-3}$)	−0.596 and 1.288	−0.395 and 0.630

[a] $R_1 = \Sigma||F_o| - |F_c||/\Sigma|F_o|$; $wR_2 = \{\Sigma[w(F^2_o - F^2_c)^2/\Sigma[w(F^2_o)^2]\}^{1/2}$. [b] $F_o > 4\sigma(F_o)$.

We have previously reported that compound **2** inhibits LPO-catalyzed iodination/oxidation reactions mainly by reducing the H_2O_2 present in the assay mixture.[33] This observation leads to an assumption that compound **2** may be oxidized to the corresponding diselenide **5** by the LPO/H_2O_2 system. As mentioned in the introduction, antithyroid drugs are oxidized by the TPO/H_2O_2 system and the resulting oxidized drugs form stable D−A complexes with either I_2 or activated iodine (I^+, produced by TPO/H_2O_2/I^-). As the oxidized drug molecules may react further with TPO/H_2O_2/I^- system in vivo to form some other metabolites, it is important to identify the metabolites produced in the reaction of antithyroid drugs with the TPO/H_2O_2/I^- system. To investigate the active metabolites of selones in the TPO-catalyzed iodination reactions, compound **3** was treated with the LPO/H_2O_2/I^- system in phosphate buffer at pH 7.4, which is similar to the assay condition of LPO-catalyzed iodination reactions.[34] It should be mentioned that LPO has been shown to behave very similarly to TPO toward iodination of thyroglobulin and other iodide acceptors. The reaction of selone **3** with the LPO/H_2O_2/I^- system produced bright orange crystals upon slow evaporation of the solvent. X-ray crystal

Table 4. Crystallographic Data for Compounds 11 and 12

	compound **11**	compound **12**
formula	$C_{11}H_{12}I_2N_2Se$	$C_{10}H_{16}N_4Se_2I_2$
F_w	502.97	603.99
crystal system	monoclinic	monoclinic
space group	*P*21/*c*	*P*21
a (Å)	14.661(7)	8.0552(8)
b (Å)	8.451(4)	11.5570(11)
c (Å)	23.808(11)	10.2634(10)
α (°)	90	90.00
β (°)	94.135(9)	107.10(2)
γ (°)	90.00	90.00
V ($Å^3$)	2942(2)	913.20(15)
D_{calc} (Mg m^{-3})	2.271	2.200
Z	8	2
μ (mm^{-1})	6.728	7.421
refl collected/unique	22367/6002	7999/4245
parameters	291	163
R_{int}	0.081	0.025
R (observed data)[a]	R_1 = 0.071; wR_2 = 0.194	R_1 = 0.031; wR_2 = 0.052
R (all data)[b]	R_1 = 0.117; wR_2 = 0.219	R_1 = 0.038; wR_2 = 0.055
goodness-of-fit on F^2	1.107	0.957
$\Delta\rho_{min}$ and $\Delta\rho_{max}$ (e $Å^{-3}$)	−1.232 and 1.565	−0.598 and 0.457

[a] $R_1 = \Sigma||F_o| - |F_c||/\Sigma|F_o|$; $wR_2 = \{\Sigma[w(F^2_o - F^2_c)^2/\Sigma[w(F^2_o)^2]\}^{1/2}$. [b] $F_o > 4\sigma(F_o)$.

Scheme 1. Synthetic Route to the Dicationic Diselenide 12 Having Two I^- as Counterions

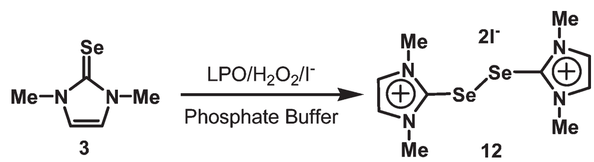

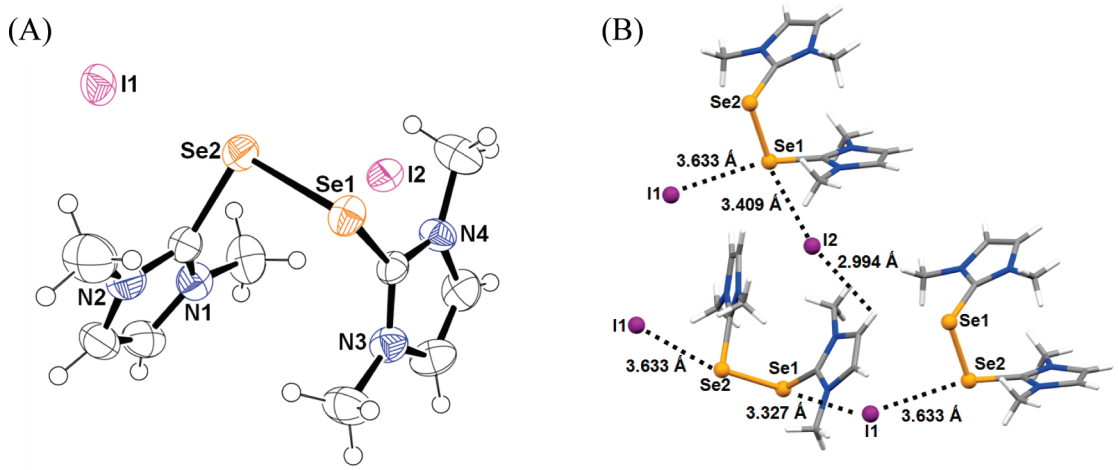

Figure 11. (A) ORTEP diagram of complex **12**, showing a dication stabilized by two I^- ions. The thermal displacement ellipsoids are shown at the 50% probability level. (B) X-ray crystal structure of **12** representing intermolecular Se···I distances as well as the H···I H-bonding interactions.

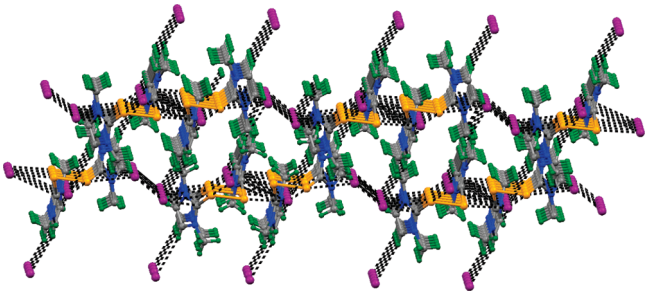

Figure 12. Packing diagram of **12** showing intermolecular Se···I and H···I interactions.

structure analysis of these crystals indicated the formation of complex **12** containing a diselenide dication and two I^- ions as counterions (Scheme 1, Figure 11A). This is in contrast to the reaction of compound **3** with I_2 in CH_2Cl_2, which produces the corresponding T-shaped charge-transfer complex having linear I−Se−I moieties.[32] Although MSeI (**2**) produces both the monocationic and dicationic species (compounds **6** and **7**) in the reaction with I_2 in aqueous medium, the reaction of selone **3** exclusively produces the corresponding dicationic diselenide **12** with two I^- as counterions in buffer.

The X-ray crystal structure of complex **12** shows some important structural features. The Se−Se bond length (2.429(8) Å) in complex **12** is significantly longer than that observed in complexes **6** (2.3821(13) Å; 2.3644(13) Å), **7** (2.3862-(6) Å), and **8** (2.3609(15) Å).[31,33] This elongation in the Se−Se bond length can be ascribed to the absence of any free N−H group in compound **12**. A similar elongation in Se−Se bond length in *N,N*-disubstituted dicationic diselenides has been observed previously.[32] Furthermore, similar to complexes **7** and **11**, complex **12** possesses some intermolecular nonbonded interactions between the Se atom and I^- ions. For example, three different Se···I intermolecular short contacts (dSe···I: 3.327 Å, 3.409 Å and 3.633 Å) were observed in compound **12**, which are much shorter than the sum of the van der Waal's radii of selenium and iodine (4.05 Å) (Figure 11B). In addition, the iodide anions are also involved in weak hydrogen bonding with the C−H group of the adjacent imidazole ring. As shown in Figure 11, I2 is hydrogen bonded to the C−H group of the neighboring imidazole ring (dI2···H5−C5: 2.994 Å; θI2···H5−C5: 147.5°). It should be mentioned that the hydrogen bonding in complex **12** is significantly different from that observed in complex **8**. Although the Br^- ions are hydrogen bonded to the free N−H group of imidazole ring in complex **8**, the I^- ions in complex **12** are hydrogen bonded to the C−H group of the imidazole ring due to the absence of free N−H group. Notably, these interactions may make a significant contribution toward the stability of these charge-transfer complexes. Similar to complex **8**, the intermolecular Se···I and H···I interactions in complex **12** assist the Se centers to adopt approximately square planar coordination geometry as shown in Figure 11. The repeated short contacts involving Se···I and H···I interactions lead to the formation of a chain-like layered structure as shown in the packing diagram of **12** (Figure 12).

CONCLUSIONS

This study shows that the selenium analogue of antithyroid drug MSeI produces different types of novel complexes in the reactions with Br_2 or I_2. The nature of complexes mainly depends on the molar ratio of MSeI to halogen. A simple substitution at the free N−H group in MSeI alters its reactivity toward Br_2 and I_2. The *N,N*-disubstituted selones exclusively produce the corresponding 10-Se-3 hypervalent "T-shaped" complexes in the reaction with Br_2 or I_2. The X-ray crystal structures of the CT complexes indicate the existence of different intermolecular Se···X (X = Br, I) and H···X (X = Br, I) interactions. The isolation and structural characterization of these CT complexes may be helpful in understanding the mechanism of antithyroid action of thiourea-based compounds.

EXPERIMENTAL SECTION

All reactions were carried out under N_2 atmosphere using Schlenk techniques. Compounds **2**, **3**, and **4** were synthesized following the literature methods.[33,34,39] FT-Raman spectra were obtained in Bruker RFS 100/S FT-Raman spectrometer.

Synthesis of Complex 8. In a 100 mL two-neck round-bottom flask fitted with a N_2 line and magnetic stirrer were placed H_2O (20 mL) and diselenide **5** (100 mg, 0.31 mmol). Dry nitrogen gas was bubbled through the solution to remove any dissolved oxygen. This solution was treated with solid sodium borohydride (26 mg, 0.70 mmol) at room

temperature. After the mixture was stirred for 30 min, the reaction mixture was extracted with deoxygenated dichloromethane (20 mL). This solution containing compound **MSeI** (0.62 mmol, assuming 100% conversion) was cooled to ~5 °C and then added dropwise with bromine (25 mg, 0.16 mmol) via syringe. The resultant orange colored, heterogeneous mixture was stirred for 1 h at ~5 °C. The solvent was removed under reduced pressure to afford an orange solid. Crystals suitable for single crystal X-ray diffraction study were obtained from a dichloromethane solution by slow evaporation method. Yield: 95 mg (62%).

Synthesis of Complex 10. To a solution of **4** (100 mg, 0.39 mmol) in CH_2Cl_2 (10 mL) was added a solution of Br_2 (65 mg, 0.39 mmol) in CH_2Cl_2 (25 mL) dropwise under nitrogen at 0 °C. The red brown solution was stirred at room temperature for 3 h. The resulting solution was concentrated to afford a red brown solid product in a quantitative yield. The product was recrystallized from CH_2Cl_2 to obtain black crystals. Yield: 80 g (76%).

Synthesis of Complex 11. To a solution of **4** (100 mg, 0.39 mmol) in CH_2Cl_2 (10 mL) was added a solution of I_2 (99 mg, 0.39 mmol) in CH_2Cl_2 (25 mL) dropwise under nitrogen at 0 °C. The red brown solution was stirred at room temperature for 3 h. The resulting solution was concentrated to obtain a red brown solid product in a quantitative yield. The product was recrystallized from CH_2Cl_2 to afford black crystals. Yield: 90 g (80%).

Synthesis of Complex 12. To a solution LPO/H_2O_2/KI in phosphate buffer (50 mM, pH 7.4),[40] a methanolic solution of compound **3** was added dropwise with stirring. The final mixture was allowed to stand at room temperature for slow evaporation of the solvent. Upon evaporation of the solvent, bright orange crystals were obtained.

X-ray Crystallography. X-ray crystallographic studies were carried out on a Bruker CCD diffractometer with graphite-monochromatized Mo−Kα radiation (λ = 0.71073 Å) controlled by a Pentium-based PC running on the SMART software package.[41−44] Single crystals were mounted at room temperature on the ends of glass fibers and data were collected at room temperature. The structures were solved by direct methods and refined using the SHELXTL software package.[42,43] All non-hydrogen atoms were refined anisotropically and hydrogen atoms were assigned to idealized locations. Empirical absorption corrections were applied to all structures using SADABS.[45] The structures were solved by direct method (SIR-92)[46] and refined by full-matrix least-squares procedure on F^2 for all reflections (SHELXL-97).[42−44]

■ ASSOCIATED CONTENT

Supporting Information. X-ray crystallographic information files (CIF) of complexes **8** and **10**−**12**. This information is available free of charge via Internet at http://pubs.acs.org.

■ AUTHOR INFORMATION

Corresponding Author
*E-mail: mugesh@ipc.iisc.ernet.in.

■ ACKNOWLEDGMENT

This study is supported by the Department of Science and Technology (DST), New Delhi, India. G.M. acknowledges the DST for the award of Swarnajayanti fellowships, and G.R. and K. P.B. thank the Council of Scientific and Industrial Research (CSIR) for their research fellowships.

■ REFERENCES

(1) Davidson, B.; Soodak, M.; Neary, J. T.; Strout, H. V.; Kieffer, J. D.; Mover, H.; Maloof, F. *Endocrinology* **1978**, *103*, 871.
(2) Taurog, A.; Dorris, M. L. *Endocrinology* **1988**, *122*, 592.
(3) Taurog, A. *Endocrinology* **1976**, *98*, 1031.
(4) Taurog, A.; Dorris, M. L.; Guziec, F. S., Jr. *Endocrinology* **1989**, *124*, 30.
(5) Taurog, A.; Dorris, M. L.; Lamas, L. *Endocrinology* **1974**, *94*, 1286.
(6) Nakashima, T.; Taurog, A.; Riesco, G. *Endocrinology* **1978**, *103*, 2187.
(7) Engler, H.; Taurog, A.; Nakashima, T. *Biochem. Pharmacol.* **1982**, *31*, 3801.
(8) Lee, E.; Miki, Y.; Katsljra, H.; Kariya, K. *Biochem. Pharmacol.* **1990**, *39*, 1467.
(9) Taurog, A.; Howells, E. *J. Biol. Chem.* **1966**, *241*, 1329.
(10) Engler, H.; Taurog, A.; Luthy, C.; Dorris, M. L. *Endocrinology* **1983**, *112*, 86.
(11) Shiroozu, A.; Taurog, A.; Engler, H.; Dorris, M. L. *Endocrinology* **1983**, *113*, 362.
(12) Magnusson, R. S.; Taurog, A. *Biochem. Biophys. Res. Commun.* **1983**, *112*, 475.
(13) Magnusson, R. P.; Taurog, A.; Dorris, M. L. *J. Biol. Chem.* **1984**, *259*, 13783.
(14) Magnusson, R. P.; Taurog, A.; Dorris, M. L. *J. Biol. Chem.* **1984**, *259*, 197.
(15) Doerge, D. R. *Biochemistry* **1986**, *25*, 4724.
(16) Doerge, D. R. *Arch. Biochem. Biophys.* **1986**, *244*, 678.
(17) Doerge, D. R. *Biochemistry* **1988**, *27*, 3697.
(18) Buxeraud, J.; Absil, A. C.; Claude, J.; Raby, C.; Catanzano, G.; Beck, C. *Eur. J. Med. Chem.* **1985**, *20*, 43.
(19) Raby, C.; Lagorce, J. F.; Jambut-Absil, A. C.; Buxeraud, J.; Catanzano, G. *Endocrinology* **1990**, *126*, 1683.
(20) Lagorce, J.; Buxeraud, J.; Jambut-Absil, A.; Raby, C. *Heterocycles* **1990**, *31*, 1609.
(21) Jambut-Absil, A.; Buxeraud, J.; Lagorce, J.; Raby, C. *Int. J. Pharm.* **1987**, *35*, 129.
(22) For further details about charge-transfer (CT) in the context of the complexes under discussion here, see Aragoni, M. C.; Arca, M.; Demartin, F.; Devillanova, F. A.; Garau, A.; Isaia, F.; Lippolis, V.; Verani, G. *Coord. Chem. Rev.* **1999**, *184*, 271.
(23) Cristiani, F.; Devillanova, F.; Isaia, F.; Lippolis, V.; Verani, F. *Polyhedron* **1995**, *14*, 2937.
(24) Aragoni, M. C.; Arca, M.; Demartin, F.; Devillanova, F.; Garau, A.; Isaia, F.; Lelj, F.; Lippolis, V.; Verani, G. *Chem.—Eur. J.* **2001**, *7*, 3122.
(25) (a) Aragoni, M. C.; Arca, M.; Demartin, F.; Devillanova, F. A.; Garau, A.; Isaia, F.; Lippolis, V.; Verani, G. *J. Am. Chem. Soc.* **2002**, *124*, 4538. (b) Arca, M.; Aragoni, M. C.; Devillanova, F.; Garau, A.; Isaia, F.; Lippolis, V.; Mancini, A.; Verani, G. *Bioinorg. Chem. Appln.* **2006**, 1.
(26) Demartin, F.; Devillanova, F. A.; Isaia, F.; Lippolis, V.; Verani, G. *Inorg. Chem.* **1993**, *32*, 3694.
(27) Demartin, F.; Devillanova, F.; Garau, A.; Isaia, F.; Lippolis, V.; Verani, G. *Polyhedron* **1999**, *18*, 3107.
(28) (a) Nosco, D. L.; Heeg, M. J.; Glick, M. D.; Elder, R. C.; Deutsch, E. *J. Am. Chem. Soc.* **1980**, *102*, 7784. (b) Daga, V.; Hadjikakou, S. K.; Hadjiliadis, N.; Kubicki, M.; dos Santos, J. H. Z.; Butler, I. S. *Eur. J. Inorg. Chem.* **2002**, *2002*, 1718. (c) Antoniadis, C. D.; Hadjikakou, S. K.; Hadjiliadis, N.; Kubicki, M.; Butler, I. S. *Eur. J. Inorg. Chem.* **2004**, *2004*, 4324. (d) Antoniadis, C. D.; Hadjikakou, S. K.; Hadjiliadis, N.; Kubicki, M.; Butler, I. S. *New. J. Chem.* **2005**, *29*, 714. (e) Corban, G. J.; Hadjikakou, S. K.; Hadjiliadis, N.; Kubicki, M.; Tiekink, E. R. T.; Butler, I. S.; Drougas, E.; Kosmas, A. M. *Inorg. Chem.* **2005**, *44*, 8617.
(29) Purcell, K. F.; Kotz, J. C. *Inorganic Chemistry*; Saunders: Philadelphia, PA, 1977; p 209.
(30) Jemmis, E. D.; Giju, K. T.; Leszczynski, J. *J. Phys. Chem.*, **1997**, *101*, 7389.
(31) Roy, G.; Nethaji, M.; Mugesh, G. *Org. Biomol. Chem.* **2006**, *4*, 2883.
(32) Bigoli, F.; Demartin, F.; Deplano, P.; Devillanova, F.; Isaia, F.; Lippolis, V.; Mercuri, M.; Pellinghelli, M.; Trogu1c, E. *Inorg. Chem.* **1996**, *35*, 3194.

(33) Roy, G.; Das, D.; Mugesh, G. *Inorg. Chim. Acta* **2007**, *360*, 303.
(34) Roy, G.; Nethaji, M.; Mugesh, G. *J. Am. Chem. Soc.* **2004**, *126*, 2712.
(35) Antoniadis, C. D.; Corban, G. J.; Hadjikakou, S. K.; Hadjiliadis, N.; Kubicki, M.; Butler, I. S. *Eur. J. Inorg. Chem.* **2003**, *2003*, 1635.
(36) Vasiliki Daga, S.; Nick Hadjiliadis, M. *Eur. J. Inorg. Chem.* **2002**, *2002*, 1718.
(37) Antoniadis, C.; Hadjikakou, S.; Hadjiliadis, N.; Papakyriakou, A.; Baril, M.; Butler, I. *Chem.—Eur. J.* **2006**, *12*, 6888.
(38) Antoniadis, C. D.; Hadjikakou, S. K.; Hadjiliadis, N.; Kubicki, M.; Butler, I. S. *Eur. J. Inorg. Chem.* **2004**, 4324.
(39) Roy, G.; Mugesh, G. *J. Am. Chem. Soc.* **2005**, *127*, 15207.
(40) Taurog, A.; Dorris, M. L.; Hu, W. X.; Guziec, F. S., Jr. *Biochem. Pharmacol.* **1995**, *49*, 701.
(41) *SMART V5.05 Software for the CCD Detector System*; Bruker Analytical X-Ray Systems, Inc.: Madison, WI, 1998.
(42) Sheldrick, G. M. *SHELXL97: A Program for Automatic Solution of Crystal Structures*, Release 97-2; University of Goettingen: Germany, 1997.
(43) Sheldrick, G. M. *SHELXTL/PC*, Version 5.03; Siemens Analytical Xray Instruments, Inc.: Madison, Wisconsin, USA, 1994.
(44) Johnson, C. K. *ORTEP-III*, Report ORNL-5138; Oak Ridge National Laboratory: Oak Ridge, TN, 1976.
(45) Sheldrick, G. M. *SADABS, A Program for Absorption Correction with the Siemens SMART Area-Detector System*; University of Goettingen: Germany. 1996.
(46) Altomare, A.; Burla, M. C.; Camalli, M.; Cascarano, G. L.; Giacovazzo, C.; Guagliardi, A.; Moliterni, A. G. G.; Polidori, G.; Spagna, R. *J. Appl. Crystallogr.* **1999**, *32*, 115.